

RESEARCH ARTICLE

Personalized 3D-printed amniotic fornical ring for ocular surface reconstruction

Nan Zhang[†], Ruixing Liu[†], Xiaowu Liu, Songlin Hou, Runan Dou, Xingchen Geng, Yan Li, Jingguo Li*, Lei Zhu*, Zhanrong Li*

Henan Eye Hospital, Henan Provincial People's Hospital, People's Hospital of Zhengzhou University, Zhengzhou 450003, China

Abstract

In the present work, we used three-dimensional (3D) printing technology to make a polylactic acid (PLA) amniotic fornical ring (AFR) for ocular surface reconstruction. This work is a retrospective and interventional case series of patients with ocular surface diseases who underwent either personalized 3D-printed AFR-assisted amniotic membrane transplantation (AMT) or sutured AMT (SAMT). Patient epidemiology, treatment, operative duration, epithelial healing time, retention time, vision changes, morbidity, and costs were analyzed. Thirty-one patients (40 eyes) and 19 patients (22 eyes) were enrolled in the 3D-printed AFR group and the SAMT group, respectively. The clinical indications of AFR and SAMT were similar, such as corneal and/or conjunctival epithelial defects due to chemical burns, thermal burns, Stevens–Johnson syndrome (SJS), or toxic epidermal necrolysis (TEN). The mean dissolution time was 15 ± 11 days in the AFR group, compared with 14 ± 7 days in the SAMT group. The percentage of healed corneal area was 90.91% (66.10%–100.00%) for AFR and 93.67% (60.23%–100.00%) for SAMT. The median time for corneal epithelial healing was 14 (7–75) days in the AFR group and 30 (14–55) days in the suture AMT group. There were no significant differences in the initial visual acuity, final visual acuity, or improvement in visual acuity between the two groups. The operation duration in the AFR group was significantly shorter than that in the SAMT group. Regarding the cost analysis, the average cost per eye in the AFR group was significantly lower than that in the SAMT group. Furthermore, 3D-printed and sterile AFR showed no obvious side effects on the eyes. Our results suggested that 3D-printed PLA scaffolds could be used as an AFR device for ocular surface disease. In addition, personalized 3D-printed AFR is superior to conventional AMT in operation duration and cost effectiveness, thereby reducing the financial burden on our health care system.

Keywords: 3D printing; Amniotic fornical ring; Amniotic membrane transplantation; Ocular surface disease

1. Introduction

The amniotic membrane (AM) from the innermost placenta is structurally divided into three layers, including the epithelium, basement membrane, and mesenchymal layer. AMs without blood vessels exhibited low immunogenicity^[1]. Amniotic membrane

[†]These authors contributed equally to this work.

***Corresponding authors:**

Jingguo Li
(lijingguo@zzu.edu.cn)

Lei Zhu
(hnyks135@126.com)

Zhanrong Li
(lizhanrong@zzu.edu.cn)

Citation: Zhang N, Liu R, Liu X, *et al.*, 2023, Personalized 3D-printed amniotic fornical ring for ocular surface reconstruction. *Int J Bioprint*, 9(3): 713. <https://doi.org/10.18063/ijb.713>

Received: November 24, 2022

Accepted: January 26, 2023

Published Online: March 20, 2023

Copyright: © 2023 Author(s). This is an Open Access article distributed under the terms of the Creative Commons Attribution License, permitting distribution and reproduction in any medium, provided the original work is properly cited.

Publisher's Note: Whioce Publishing remains neutral with regard to jurisdictional claims in published maps and institutional affiliations.

transplantation (AMT) promotes epithelialization by facilitating corneal and conjunctival cell migration. Meanwhile, AMs can secrete several cytokines and inhibit inflammation, scarring and angiogenesis^[2]. Since the 1940s, AM has been most commonly used in ocular surface reconstruction due to a variety of diseases, including chemical burns, pterygium, ocular surface neoplasia, Steven–Johnson syndrome (SJS), and toxic epidermal necrolysis (TEN)^[3].

The AM is only approximately 0.1 mm thick. The AM is so thin that it is prone to intraoperative tears and early postoperative dissolution. Moreover, prolonged sutures can induce conjunctival granulomas. ProKera, which is a cryopreserved AM that is installed upon polycarbonate ring systems, has been approved by the United States Food and Drug Administration (U.S. FDA)^[4]. The advantages of ProKera over traditional sutured AM are that there is no need for sutures or operating rooms, and it is easy to insert and remove. Zhou *et al.* reported that ProKera prolonged the dissolution time compared with that of sutured AMT^[5]. If an extensive ocular surface injury occurs, the AM is required to cover the entire ocular surface, including the cornea, bulbar conjunctiva, palpebral conjunctiva, conjunctival vault, and palpebral margin. However, the ProKera device can only cover the cornea and perilimbal conjunctiva. In addition, edema of the conjunctiva and eyelids often occurs in the acute stage of the disease, resulting in difficult exposure of the operative field, prolonging the suture time, and increasing the risk of surgery for patients. Therefore, it is necessary to develop a new device to facilitate AM fixation in the conjunctival vault or even cover the eyelid margin.

In recent years, three-dimensional printing (3DP) technology has been widely applied in medicine and include implants, medical instruments, prosthetics, and pharmaceutical products. 3DP has enormous potential in fabricating customized, low-cost, and complex scaffolds^[6]. 3DP membranes, as an alternative to amniotic membranes, have also been used for ocular surface or conjunctival defect reconstruction^[7]. Fused deposition modeling (FDM), which is one of the most commonly used 3DPs, is a complex process, including drawing the solid filament into the printer head, melting in the heating zone, and extruding through the printer nozzle. FDM has several advantages, including flexibility, having a wide range of materials, being economical, and personalized precision^[8]. Polylactic acid (PLA) has become the most frequently utilized 3D-printed material because of its low cost and relatively low melting point. Moreover, it has been approved as a biomedical material due to its good biocompatibility^[9]. In the present study, we fabricated personalized amniotic fornical rings (AFRs) with PLA materials by 3DP technology according to different

conjunctival sac sizes. The purpose of this retrospective analysis is to collect related material and detailed clinical information from enrolled patients. In particular, we explored the clinical indications of AFR and compared the outcomes with those of SAMT. Moreover, the cost-effectiveness was analyzed between the SAMT and AFR groups.

2. Materials and methods

2.1. Materials

PLA 3DP Filament (diameter: 1.75 mm) was purchased from Sigma-Aldrich (USA). A HORI Z300 PLUS 3D printer was purchased from Huitianwei Technology Co., Ltd. (Beijing, China). Oxybuprocaine hydrochloride eye drops (0.4%, 20 mL, Santen, Japan) were used as a topical anesthetic. Lidocaine hydrochloride injection (2%, Sinopharm Ronshyn Pharmaceutical Co., Ltd. China) was used for infiltration anesthesia. Topical medications, including eye gel of deproteinized calf blood extract (20%, 5 g, Shenyang Xingqi Pharmaceutical Co., Ltd.), sodium hyaluronate eye drops (0.1%, 10 mL, Germany), levofloxacin eye drops (0.5%, Santen, Japan), gatifloxacin eye gel (0.3%, 5 g, Shenyang Xingqi Pharmaceutical Co., Ltd.), TobraDex eye drops (tobramycin 0.3% and dexamethasone 0.1%, 5 mL, Alcon, USA), TobraDex eye ointment (tobramycin 0.3% and dexamethasone 0.1%, 3.5 g, Alcon, USA), and Tacrolimus eye drops (0.1%, Santen, Japan) were used to promote epithelial repair, prevent infection, and alleviate inflammation, respectively. A 10-0 nylon suture (Alcon, USA) was used to secure the amniotic membrane.

2.2. Fabrication of sterile AFR

The 3D-printed AFR was designed with Autodesk 123D design software. The STL files were converted to the gcode format using CURA software. PLA filaments were loaded into the 3D printer, melted at 210°C and extruded through a nozzle (0.4 mm) to print layer by layer. The layer height and the printing speed were 0.2 mm and 60 mm/s, respectively. The wall thickness of the AFR is 0.8 mm. The transverse and longitudinal diameters of the AFR are based on the size of the patients' conjunctiva sac. The fabrication of the AFR is illustrated in Figure 1A. The AFR was sterilized with ethylene oxide before surgery. The acute phase of inflammation often leads to massive exudation in the conjunctival sac. Therefore, in patients who are in the acute phase, the AFR needs to be partially clipped to leave a gap for exudates to drain (Figure 1A).

2.3. Description of technique

Ethics approval was obtained from Henan Eye Hospital (Permit number: HNEEC-2022(53)). The institutional review board approved a retrospective medical review of patients, who underwent AFR and suture AMT (SAMT) for various ocular surface injuries between January 2019

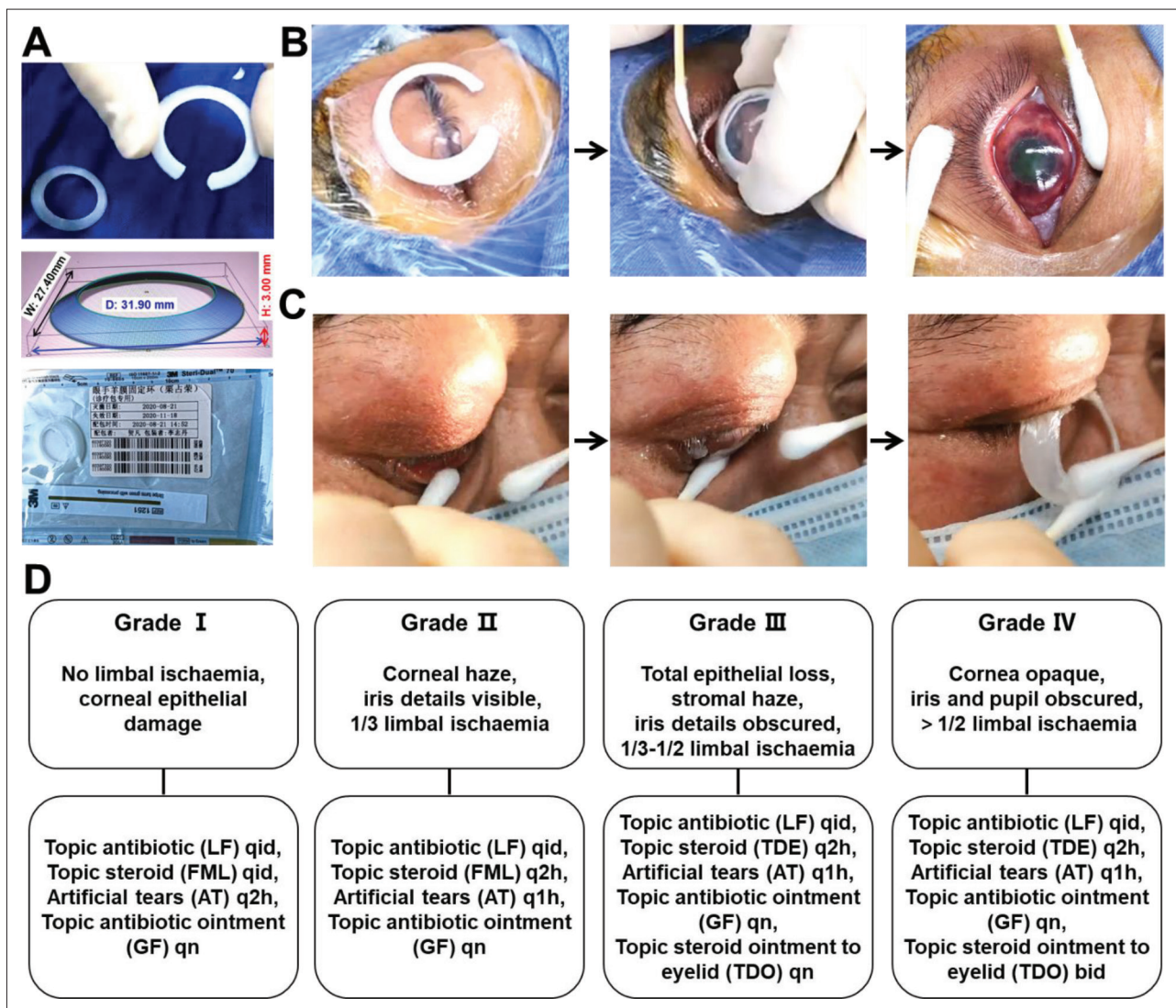


Figure 1. (A) The 3D-printed design and a photograph of the amniotic fornical ring. The physical image of trimmed 3D-printed AFR; software design diagram of AFR; image of AFR after disinfection with ethylene oxide. (B) Implantation procedures of 3D-printed AFR. The AFR was placed on the unfolded AM (40 × 60 mm). The AM with an enclosed AFR was slipped into the conjunctival sac after gently turning the upper and lower eyelids. (C) The removal procedures of AFR. (D) Diagram outlining the protocol for medication of ocular manifestations in acute ocular burns according to Roper-Hall grades.

and July 2022. Only patients with follow-up ≥ 2 weeks after AM were included. Written informed consent was signed by each patient or legal guardian.

First, the doctor measured the size of the conjunctival sac as described previously^[10]. Briefly, the distance between the superior and inferior fornical rims was measured as the outer diameter of the AFR transverse diameter. The distance between the nasal and temporal fornical rims was taken as the outer diameter of the AFR longitudinal diameter. Appropriate and sterile AFR was selected. Next, AFR-assisted AMT was performed under surface anesthesia or nerve block anesthesia depending on the patient's general condition. Briefly, the operation was

performed according to the routine aseptic procedure^[11]. If necessary, the exudate or any residual foreign body was removed from the conjunctival sac. Then, the AFR was placed on the expanded cryopreserved AM (40 × 60 mm). The AM with an enclosed AFR was inserted into the conjunctival sac after gently turning the superior and inferior eyelids. It was ensured that the AFR reached the fornices without causing lagophthalmos. In the patients with SJS or TEN, it was required that the AM covered the damaged cornea, conjunctiva, and eyelid margin due to the widespread epithelial defects of the ocular surface and eyelid margin. The AFR application methods are shown in [Figure 1B](#). The AM was anchored to the external eyelid skin with sutures if necessary. The AM was sutured with

10-0 nylon sutures to the ocular surface in the conventional SAMT group. When the AM dissolved and could not cover the defective keratoconjunctival epithelium, the AFR, AM, or suture was removed. The AFR were removed by gently pulling the lower eyelid (Figure 1C). All eyes received topical medications (see Figure 1D). The patients with severe chemical injuries received the administration of intravenous dexamethasone and vitamin C if necessary. The patients with SJS or TEN were administered tacrolimus eye drops topically in addition to the above treatments.

2.4. Parameter estimation

The collected data included age, sex, etiology, affected eye, degree of chemical burns, patient symptoms, visual acuity (VA), intraocular pressure (IOP), ophthalmological findings, epithelial defect healing, complications, time of AFR or AM retention, and follow-up. The patient symptoms were recorded based on subjective reports at each visit and slit-lamp examination. VA was assessed using a fractional eye chart at each visit and subsequently converted to logMAR values for analysis. “Counting Fingers” were rated by LogMAR 2.0, and “Hand Movements” were rated by LogMAR 2.3. If the patient’s VA was light perceptive, the patient was excluded from the statistical analysis^[12]. The degree of ocular surface burns was graded according to the Roper-Hall and Dua classifications^[13,14]. The patients with SJS or TEN were graded according to previous literature^[15]. The grading standard of symblepharon was referred to in previous literature^[16]. Note that all patients were administered levofloxacin eye drops four times per day as prophylaxis.

The percentage of healed corneal area (PHCA) was defined as described in previous literature^[5], i.e., $PHCA = (\text{final area} - \text{initial area}) / \text{initial area} \times 100\%$. We assessed the final corneal epithelial defect area by fluorescein staining when AFR or dissolution of AM was removed. In the cost-effective analysis, the cost for 1% healing area was defined as total cost/PHCA. Data are shown as mean \pm SD or median (range).

2.5. Statistical analysis

Data analysis was performed with SPSS 25.0. The results are shown as the mean \pm SD or median (interquartile range, the 25th percentiles–the 75th percentiles) with a significance level of 0.05. To compare collected data with baseline data, chi-square test or Fisher’s exact test was used for qualitative data. Independent *t*-tests or Mann–Whitney *U* tests were used for quantitative data.

3. Results and discussion

From January 2019 to July 2022, 62 eyes of 50 patients (2–89 years old) were screened, and the eye conditions included alkaline chemical burns, acidic chemical burns,

Table 1. Demographics and characteristics of patients

	AFR	SAMT	<i>P</i>
Sex (F:M)	5 : 26	2 : 17	
Age (years, range)	46 \pm 17 (9–89)	38 \pm 22 (2–70)	0.187
Indications			
Acid	2 (5%)	3 (13.6%)	
Alkali	25 (62.5%)	12 (54.5%)	
Thermal	7 (17.5)	7 (31.9%)	
SJS and TEN	6 (15%)	0	
Time of presentation (days)			
0–1	10 (25%)	5 (22.7%)	
2–7	20 (50%)	8 (36.4%)	
>7	10 (25%)	9 (40.9%)	
Roper-Hall classification			
I	12 (35.3%)	4 (18.2%)	
II	5 (14.7%)	6 (27.3%)	
III	6 (17.6%)	8 (36.4%)	
IV	11 (32.4%)	4 (18.2%)	
Dua’s classification			
I	12 (35.3%)	4 (18.2%)	
II	5 (14.7%)	6 (27.3%)	
III	6 (17.6%)	8 (36.4%)	
IV	6 (17.6%)	3 (13.6%)	
V	3 (8.8%)	0	
VI	2 (5.9%)	1 (4.5%)	
Additional treatments			
PKP	1 (2.5%)	0	
Tarsorrhaphy	8 (20%)	3 (13.6%)	
Bandage contact lens	9 (22.5%)	4 (18.2%)	
Total number of eyes	n = 40	n = 22	
Burned by chemical and heat	n = 34	n = 22	

Abbreviations: AFR, amniotic fornical ring; PKP, penetrating keratoplasty; SAMT, sutured amniotic member transplant; SJS, Stevens-Johnson syndrome; TEN, toxic epidermal necrolysis.

thermal burns, SJS, and TEN. Alkaline burns were the most common cause of ocular surface damage. Data from 40 eyes of 31 patients (5 female and 26 male) were collected in the AFR group. In the SAMT group, 22 eyes of 19 patients (2 female and 17 male) were analyzed. The mean age was 46 \pm 17 years (range: 9–89 years) in the AFR group and 38 \pm 22 years (range: 2–70 years) in the SAMT group (Table 1). There was no significant difference in patient age between the two groups. The main indications for using AFR and SAMT were similar and mainly included ocular surface burns. Six patients with SJS or TEN underwent AFR-assisted AMT. Notably, AFR can be used alone in

SJS and TEN with extended ocular surface damage. Here, we provided some eye pictures of patients with AFR, including TEN, thermal burn, acid burn, and alkaline burns (Figure 2). Moreover, we showed a long follow-up of patients with TEN who received AFR (Figure 2C). Figure 2A shows extensive exudation in the conjunctival sac and widespread ocular surface epithelial and palpebral margin defects in an intensive care unit patient with TEN before AFR-assisted AMT. AFR supported the AM to the fornices and kept the eyelid closed. Meanwhile, the AM covered the superior and inferior eyelid skin several millimeters away from the eyelid margin. The AM had dissolved at 3 weeks after surgery in two eyes. The corneal epithelium of the right eye had healed completely, while the corneal epithelium of the left eye still had a flaky defect at 3 weeks after surgery. At this time, the epithelium of the double eyelid margin was still not completely repaired (Figure 2A). Figure 2B demonstrates that the cornea was completely clear despite a punctured epithelial defect in the right eye. The cornea presented with scattered punctate epithelial defects, and there was a slight opacity in the left eye at 3 months after the operation (Figure 2B). At the same time, the eyelid margin also showed moderate congestion and inflammation (Figure 2B). The cornea of the right eye was clear, and the corneal opacity of the left eye was significantly reduced 9 months after surgery (Figure 2C). The best corrected VA was 1.0 for the right eye and 0.5 for the left eye 9 months after surgery. However, ProKera, another sutureless AM mounted device, is approximately 16 mm in diameter and can only cover the cornea and peripheral sclera. Therefore, it cannot be used alone in patients with widespread ocular surface and eyelid injuries, such as SJS and TEN^[5]. AFR can be used alone for widespread ocular surface and eyelid injuries, and its effect is related to supporting AM to the conjunctival fornix. It may be that just the AFR had the ability to extend and immobilize the AM more fully. Three patients complained of mild foreign body sensation in the early postoperative period, followed by a significant reduction in discomfort and disappearance.

The median initial VA was 0.959 (0.600–1.775) for the AFR group and 1.150 (0.700–2.000) for the SAMT group. During post-treatment follow-up, the median final VA was 0.300 (0.100–0.900) (AFR) and 0.450 (0.300–1.200) (SAMT). The VA improvement was 0.400 (0.200–0.900) in the AFR group and 0.500 (0.200–0.800) in the SAMT group (Table 2). There was no significant initial or final VA difference between the two groups. The median dissolution or removal times were 7 (7–19) days in the AFR group and 14 (7–14) days in the SAMT group ($P = 0.812$, Table 2). The mean time of dissolution or removal was 15 ± 11 days in the AFR group and 14 ± 7 days in the SAMT group

($P = 0.812$, Table 2). In our study, the AM dissolution time was shorter than that reported in the literature^[5]. The thickness of the AM was also one of the main factors affecting AM dissolution^[2]. AFR and suture had similar dissolution times as that for the AM. Therefore, we speculated that the shorter dissolution time may be related to the thin AM. The percentages of healed surface area were 90.91% (66.10%–100.00%) for AFR and 93.67% (60.23%–100.00%) for SAMT ($P = 0.994$). The median epithelial healing time was 14 (7–75) days for AFR and 30 (14–55) days for SAMT ($P = 0.436$, Table 2). The average epithelial healing time was 44 ± 52 days for AFR and 40 ± 41 days for SAMT ($P = 0.751$, Table 2). The incidence of symblepharon was 31.58% for AFR and 40.91% for SAMT ($P = 0.465$). Limbal stem cell deficiency accounted for 31.58% in the AFR group and 54.55% in the SAMT group ($P = 0.080$). No conjunctival granulomas occurred in the AFR group, although there was no difference in the incidence of granulomas between the AFR and SAMT groups ($P = 0.407$). Suture-induced conjunctival granuloma is a chronic inflammation caused by suture irritation. The lower incidence of conjunctival granulomas in our study may be related to the faster dissolution of the AM and the earlier removal of sutures.

Two patients in the AFR group suffered from glaucoma complications. Three patients in both the AFR and SAMT groups developed traumatic cataracts. These complications occurred in the patients with alkaline burns. We hypothesized that this might be related to the high tissue permeability of alkaline fluid and the administration of postoperative glucocorticoids^[17]. Subconjunctival effusion was observed in two patients in the acute stage of burn injury in the AFR group. The subconjunctival effusion disappeared after correct ocular nursing guidance. All enrolled patients tolerated the device during the whole treatment process. We found no associated infections.

Subsequent to the removal of 3D-printed AFR, one patient underwent penetrating keratoplasty, and eight patients underwent tarsorrhaphy. The other nine patients wore a bandage contact lens (Table 1). Three patients underwent tarsorrhaphy, and four patients needed bandage contact lens treatment after the removal of the sutured AM.

The mean operative duration (MOD) per eye was 18.4 ± 10.1 min in the AFR group and 42.2 ± 18.5 min in the SAMT group ($P = 0.000$, Table 3). The MOD per eye was 16 (10–24) min in the AFR group and 35 (30–47) min in the SAMT group ($P = 0.000$, Table 3). There were significant differences in the MOD between the two groups. Shorter operative times may be associated with bedside procedures, topical or surface anesthesia, and suture-free techniques. Several techniques have been previously

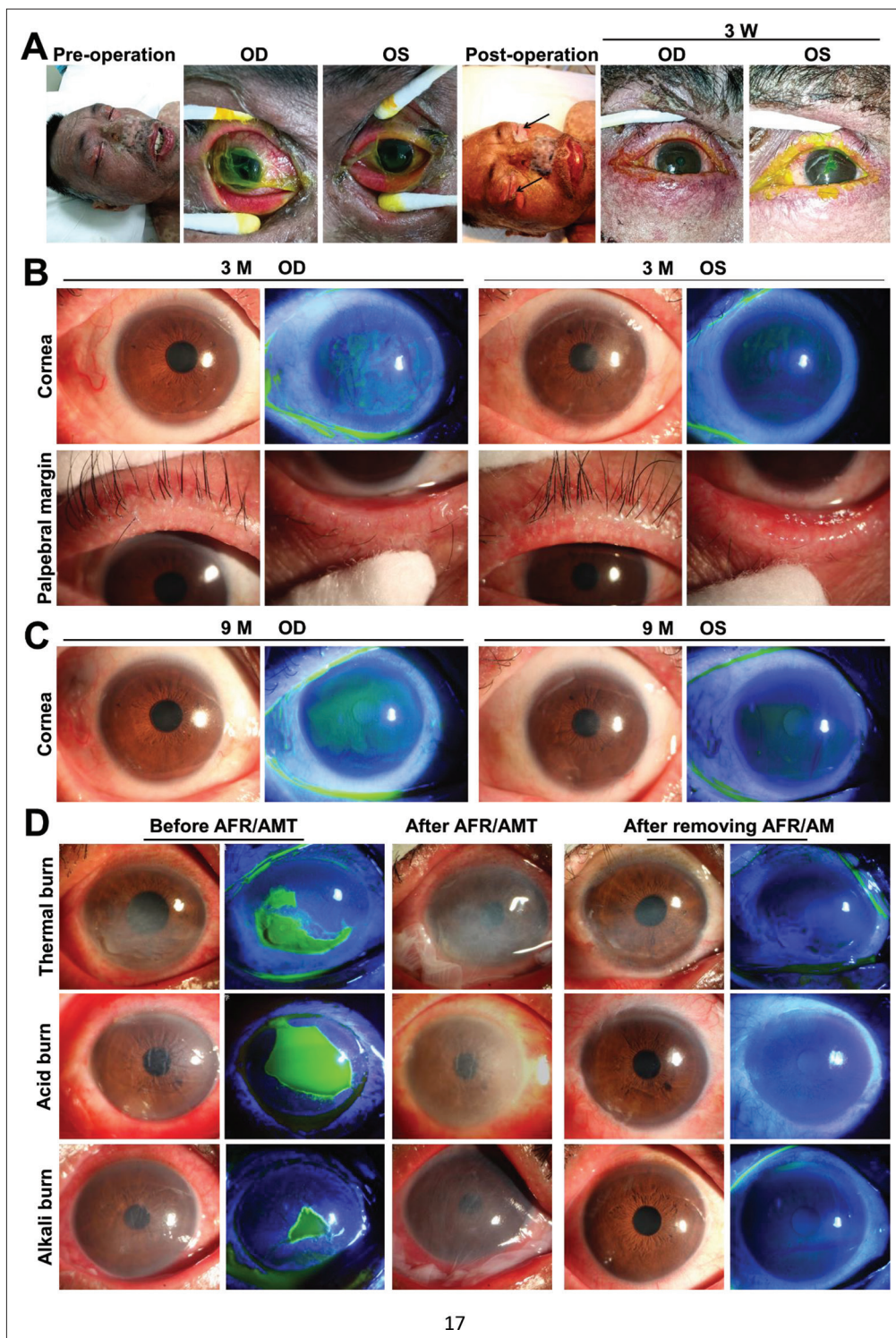


Figure 2. Photographs of patients with AFR. (A) The 9-month follow-up photographs of a patient with TEN. The AM dissolved completely in both eyes 3 weeks after surgery. The corneal epithelium healed completely in the right eye, and the defect remained at 3 × 4 mm in size in the left eye 3 weeks after surgery. (B) The cornea of the right eye had completely returned to having a normal transparency. The cornea remained slightly opaque in the left eye 3 months after the operation. The eyelid margin showed moderate congestion and inflammation. (C) The cornea of the right eye was clear, and the corneal opacity of the left eye was significantly reduced 9 months after surgery. (D) Photographs of patients with thermal, acid, and alkali burns.

Table 2. Comparison of different outcomes of the patients in two treatment groups

	AFR	SAMT	P
Initial VA (logMAR)	0.959 (0.600–1.775)	1.150 (0.700–2.000)	0.414
Final VA (logMAR)	0.300 (0.100–0.900)	0.450 (0.300–1.200)	0.214
VA improvement (initial–final) (logMAR)	0.400 (0.200–0.900)	0.500 (0.200–0.800)	0.688
Epithelial healing time (days)	14 (7–75)	30 (14–55)	0.386
	44 ± 52	40 ± 41	0.751
AM dissolution or removal time (days)	7 (7–19)	14 (7–14)	0.436
	15 ± 11	14 ± 7	0.812
The percentage of healed corneal area	90.91% (66.10%–100.00%)	93.67% (60.23%–100.00%)	0.994
Symblepharon	12 (31.58%)	9 (40.91%)	0.465
Conjunctival granuloma	0	1 (4.55%)	0.407
Limbal stem cell deficiency (LSCD)	12 (31.58%)	12 (54.55%)	0.080
Glaucoma	2 (5.26%)	0	0.508
Cataract	3 (7.89%)	3 (13.64%)	0.961

Abbreviations: AM, amniotic membrane; LSCD, limbal stem cell deficiency; VA, visual acuity.

Table 3. Cost analysis between 3D-printed AFR and SAMT

	AFR	SAMT	P
Cost analysis			
Surgeon's compensation	870.00 (734.25–979.00)	968.00 (870.00–979.00)	0.037
Sutures	0.00 (0.00–0.00)	128.63 (122.50–192.94)	0.000
Operation room cost	158.65 (128.72–257.44)	257.44 (133.67–267.90)	0.100
Anesthesia cost	40.00 (36.25–70.00)	129.00 (58.38–854.63)	0.001
Price per 1% area healed	12.79 (9.97–16.61)	19.24 (13.85–36.81)	0.001
Operation time (min)	16 (10–24)	35 (30–47)	0.000
	18.4 ± 10.1	42.2 ± 18.5	0.000

described for sutureless human amniotic fixation on the ocular surface. Researchers reported a polymethyl methacrylate (PMMA)-based ring for a therapeutic contact lens on the cornea of New Zealand rabbits^[18,19]. However, PMMA material increased the discomfort and the risk of ring slipping out. In this study, none of the personalized 3D-printed AFRs automatically slipped out of the conjunctival sac. Moreover, the 3D-printed AFR was easy to replace, similar to a contact lens. A custom-made fornical ring with sterile intravenous tubing (IVT) could cover the entire mucosal surface and eyelid^[10]. The disadvantages of the IVT ring include its time-consuming

nature and the presence of amniotic folds. The 3D-printed AFR allows the AM to fit to the ocular surface better without wrinkles (Figure 2A). Therefore, the advantages of 3D-printed AFR include its individual design, easy bedside insertion without the need for sedation, and easy replacement after AM dissolution.

Another AMT was required in 15 eyes (37.5%) in the AFR group and in 9 eyes (40.9%) in the SAMT group because of earlier AM dissolution. Regarding the cost analysis (Table 3), 3D-printed AFRs were provided free of charge. The price of AM changed during the trial, and since

all the enrolled patients required AM, the price of AM was not analyzed. The patients in the AMP group basically did not need sutures. Among them, four patients (six eyes) underwent amnion suturing at the eyelid margin due to a severe eyelid injury, especially at the upper eyelid margin. The AM was not easily attached due to the blinking reflex and gravity. The patients in the AFR group spent 0.00 (0.00–0.00) Chinese Yuan (CNY) per eye. The patients needed 1–2 sutures per eye, with a median of RMB 128.63 (122.50–192.94) CNY in the SAMT group ($P = 0.000$). Regarding preoperative anesthesia, the patients who were given AFR spent a median of 40.00 (36.25–70.00) CNY per eye. Most of the patients in the AFR group underwent AMT with local or surface anesthesia, but nongeneral anesthesia can also be used for children (<18 years old). In contrast, in most patients, nerve block anesthesia or general anesthesia was used, and the median cost per eye was 129.00 (58.38–854.63) CNY ($P = 0.001$) in the SAMT group. Regarding the surgeon's operating costs, the patients spent a median of 870 (734.25–979.00) CNY per eye in the AFR group, and the patients spent a median of 968.00 (870.00–979.00) CNY per eye in the SAMT group ($P = 0.037$). The significant difference in the operating charges between the two groups may be because some patients in the AFR group were treated at the bedside. Placement and removal of the 3D-printed AFR was a bedside procedure that saved time. Traditional SAMT requires surgery-related equipment and personnel. Hence, 3D-printed AFR represents a more economical method of ocular surface reconstruction.

3DP technology has been widely explored for tissue regeneration and wound repair. Researchers reported an *in situ* bioprinted microalgal hollow fiber scaffold with autotrophic oxygen capacity that promotes irregularly shaped wound healing^[20]. 3DP technology has also been used for corneal tissue engineering and ocular surface reconstruction. Corneal stroma regeneration can be induced by 3D fibrous hydrogel constructs injected with gelatin methacrylate^[21]. In addition, 3D-printed gelatin-based membranes showed more predictable degradability, a high goblet cell density of the healing epithelium, and less inflammatory response and scar formation. These advantages of the 3D-printed membrane make it a promising alternative to the amniotic membrane^[7]. A custom imprint 3D-scanned scleral contact lens fits the ocular surface more accurately, expands the indications for scleral contact lens, and can be used as a remedial therapy for scleral contact lens failure^[22]. In the present study, we demonstrated that 3D-printed AFR can be used for ocular surface reconstruction, and it can be performed at the bedside and greatly reduce the surgical time. 3DP

technology shows good application potential in ocular surface reconstruction.

Our study was limited by its retrospective design and the small sample size. However, this study shows benefits of this technique, including a decreased operation duration and less cost. To the best of our knowledge, 3D-printed AFR has not been reported for ocular surface diseases. This study highlights the application of 3DP technology in ocular surface reconstruction.

4. Conclusion

We successfully fabricated a novel personalized 3D-printed AFR with PLA for ocular surface reconstruction. Retrospective analysis results showed that the 3D-printed AFR was successfully applied to ocular surface diseases. The advantages of 3D-printed AFRs included its individual design, ease of use, time-saving ability, low cost, and easy replacement after AM dissolution. 3D-printed AFR has great potential for ocular surface reconstruction.

Acknowledgments

The authors would like to thank Zhuoya Yao and Junhui Geng (Disinfection Supply Center, Henan Provincial People's Hospital).

Funding

This work was supported by the National Natural Science Foundation of China (52173143 and 82101090), Project of Henan Provincial Health Department (200803096), Medical Science and Technology Project of Henan Province (SBGJ202103012) and Basic Science Key Project of Henan Eye Institute/Henan Eye Hospital (20JCZD002, 20JCQN001 and 22JCQN001).

Conflict of interest

The authors declare no conflict of interests.

Author contributions

Conceptualization: Nan Zhang, Xiaowu Liu, Yan Li, Jingguo Li, Lei Zhu, Zhanrong Li

Investigation: Nan Zhang, Ruixing Liu, Xiaowu Liu, Jingguo Li, Lei Zhu, Zhanrong Li

Methodology: Nan Zhang, Ruixing Liu, Xiaowu Liu, Songlin Hou, Runan Dou, Xingchen Geng, Yan Li, Zhanrong Li

Formal analysis: Nan Zhang, Ruixing Liu, Jingguo Li, Lei Zhu, Zhanrong Li

Writing – original draft: Nan Zhang, Jingguo Li, Zhanrong Li

Writing – review & editing: Nan Zhang, Jingguo Li, Zhanrong Li

Ethics approval and consent to participate

This study was approved by the institutional review board of Henan Eye Hospital (Permit number: HNEEC-2022(53)). The institutional review board approved a retrospective medical review of the patients who underwent AFR and suture AMT (SAMT) for various ocular surface injuries between January 2019 and July 2022. Only patients with follow-up ≥ 2 weeks after AM were included. All patients signed the informed consent form, and the permission was obtained from each of the subjects to participate in the study

Consent for publication

All patients signed the written informed consent form, and the permission was obtained from each of the subjects to publish their data and images.

Availability of data

All data that support the findings of this study have been included in the article.

References

- Mamede AC, Carvalho MJ, Abrantes AM, *et al.*, 2012, Amniotic membrane: From structure and functions to clinical applications. *Cell Tissue Res*, 349(2):447–458.
<https://doi.org/10.1007/s00441-012-1424-6>
- Finger PT, Jain P, Mukkamala SK, 2019, Super-thick amniotic membrane graft for ocular surface reconstruction. *Am J Ophthalmol*, 198:45–53.
<https://doi.org/10.1016/j.ajo.2018.09.035>
- Sangwan VS, Burman S, Tejwani S, *et al.*, 2007, Amniotic membrane transplantation: A review of current indications in the management of ophthalmic disorders. *Indian J Ophthalmol*, 55(4):251–260.
<https://doi.org/10.4103/0301-4738.33036>
- Morkin MI, Hamrah P, 2018, Efficacy of self-retained cryopreserved amniotic membrane for treatment of neuropathic corneal pain. *Ocul Surf*, 16(1):132–138.
<https://doi.org/10.1016/j.jtos.2017.10.003>
- Zhou TE, Robert MC, 2022, Comparing ProKera with amniotic membrane transplantation: Indications, outcomes, and costs. *Cornea*, 41(7):840–844.
<https://doi.org/10.1097/ICO.0000000000002852>
- Mei Y, He C, Gao C, *et al.*, 2021, 3D-printed degradable anti-tumor scaffolds for controllable drug delivery. *Int J Bioprint*, 7(4):418.
<https://doi.org/10.18063/ijb.v7i4.418>
- Dehghai S, Rasoulianboroujeni M, Ghasemi H, *et al.*, 2018, 3D-printed membrane as an alternative to amniotic membrane for ocular surface/conjunctival defect reconstruction: An in vitro & in vivo study. *Biomaterials*, 174:95–112.
<https://doi.org/10.1016/j.biomaterials.2018.05.013>
- Zhang B, Cristescu R, Chrisey DB, *et al.*, 2020, Solvent-based extrusion 3D printing for the fabrication of tissue engineering scaffolds. *Int J Bioprint*, 6(1):211.
<https://doi.org/10.18063/ijb.v6i1.211>
- Singhvi MS, Zinjarde SS, Gokhale DV, 2019, Polylactic acid: Synthesis and biomedical applications. *J Appl Microbiol*, 127(6):1612–1626.
<https://doi.org/10.1111/jam.14290>
- Ma KN, Thanos A, Chodosh J, *et al.*, 2016, A novel technique for amniotic membrane transplantation in patients with acute Stevens-Johnson syndrome. *Ocul Surf*, 14(1):31–36.
<https://doi.org/10.1016/j.jtos.2015.07.002>
- Clare G, Suleman H, Bunce C, *et al.*, 2012, Amniotic membrane transplantation for acute ocular burns. *Cochrane Database Syst Rev*, 2012(9):CD009379.
<https://doi.org/10.1002/14651858.CD009379.pub2>
- Lange C, Feltgen N, Junker B, *et al.*, 2009, Resolving the clinical acuity categories “hand motion” and “counting fingers” using the Freiburg Visual Acuity Test (FrACT). *Graefes Arch Clin Exp Ophthalmol*, 247(1):137–142.
<https://doi.org/10.1007/s00417-008-0926-0>
- Roper-Hall MJ, 1965, Thermal and chemical burns. *Trans Ophthalmol Soc U K (1962)*, 85:631–53.
- Dua HS, King AJ, Joseph A, 2001, A new classification of ocular surface burns. *Br J Ophthalmol*, 85(11):1379–1383.
<https://doi.org/10.1136/bjo.85.11.1379>
- Shanbhag SS, Hall L, Chodosh J, *et al.*, 2020, Long-term outcomes of amniotic membrane treatment in acute Stevens-Johnson syndrome/toxic epidermal necrolysis. *Ocul Surf*, 18(3):517–522.
<https://doi.org/10.1016/j.jtos.2020.03.004>
- Kheirkhah A, Blanco G, Casas V, *et al.*, 2008, Surgical strategies for fornix reconstruction based on symblepharon severity. *Am J Ophthalmol*, 146(2):266–275.
<https://doi.org/10.1016/j.ajo.2008.03.028>
- Sharma N, Singh D, Sobti A, *et al.*, 2012, Course and outcome of accidental sodium hydroxide ocular injury. *Am J Ophthalmol*, 154(4):740.e2–749.e2.
<https://doi.org/10.1016/j.ajo.2012.04.018>
- Liu BQ, Wang ZC, Liu LM, *et al.*, 2008, Sutureless fixation of amniotic membrane patch as a therapeutic contact lens by using a polymethyl methacrylate ring and fibrin sealant in a rabbit model. *Cornea*, 27(1):74–79.
<https://doi.org/10.1097/ICO.0b013e318156cb08>

19. Liang X, Liu Z, Lin Y, *et al.*, 2012, A modified symblepharon ring for sutureless amniotic membrane patch to treat acute ocular surface burns. *J Burn Care Res*, 33(2):e32–e38.
<https://doi.org/10.1097/BCR.0b013e318239f9b9>
20. Wang X, Yang C, Yu Y, *et al.*, 2022, In situ 3D bioprinting living photosynthetic scaffolds for autotrophic wound healing. *Research (Washington, D.C.)*, 2022:9794745.
<https://doi.org/10.34133/2022/9794745>
21. Kong B, Chen Y, Liu R, *et al.*, 2020, Fiber reinforced GelMA hydrogel to induce the regeneration of corneal stroma. *Nat Commun*, 11(1):1435.
<https://doi.org/10.1038/s41467-020-14887-9>
22. Silverman JIM, Huffman JM, Zimmerman MB, *et al.*, 2021, Indications for wear, visual outcomes, and complications of custom imprint 3D scanned scleral contact lens use. *Cornea*, 40(5):596–602.
<https://doi.org/10.1097/ICO.0000000000002588>